EPJ Web of Conferences **40**, 06007 (2013)
DOI: 10.1051/epjconf/20134006007

Metastable $Sm(Fe,Cu)_5$ ordered alloy films formed on Cu(111) underlayers

Takato Yanagawa[1], Mitsuru Ohtake[1], Fumiyoshi Kirino[2], and Masaaki Futamoto[1]

[1]Faculty of Science and Engineering, Chuo University, 1-13-27 Kasuga, Bunkyo-ku, Tokyo, 112-8551, Japan
[2]Graduate School of Fine Arts, Tokyo University of the Arts, 12-8 Ueno-koen, Taito-ku, Tokyo, 110-8714, Japan

Abstract. Sm-Fe thin films are prepared on Cu(111) underlayers hetero-epitaxially grown on MgO(111) single-crystal substrates by using an ultra-high vacuum molecular beam epitaxy system. The Sm/Fe composition is varied from Fe-rich (10 at. % Sm - Fe) to Sm-rich (30 at. % Sm - Fe) region including $SmFe_5$ stoichiometry. The influence of film composition on the film structure is studied by *in-situ* reflection high-energy electron diffraction and X-ray diffraction. Metastable $Sm(Fe,Cu)_5$ ordered phase formation is recognized in the Sm-Fe films with the investigated compositions. Cu atoms diffuse from the underlayer into the Sm-Fe film and substitute the Fe site in $SmFe_5$ structure forming an alloy compound of $Sm(Fe,Cu)_5$. The Sm-Fe films with Fe-rich compositions consist of $Sm(Fe,Cu)_5$ and bcc-Fe phases, whereas the Sm-Fe films with Sm-rich compositions consist of $Sm(Fe,Cu)_5$ and amorphous phases. Cu atom diffusion into Sm-Fe film is assisting the formation of ordered phase.

1 Introduction

Perpendicularly magnetized thin films with high uniaxial magnetocrystalline anisotropy energies (K_u) have attracted much attention to applications like magnetic recording media, magnetic random access memory devices, etc. $SmCo_5$ ordered alloy is a high K_u material (1.1×10^8 erg/cm^3) with $CuCu_5$-type crystal structure. $SmCo_5$ polycrystalline [1–6] and epitaxial [7–9] films with (0001) texture have been prepared by employing Cu [1–4, 8, 9], Cu/Ti [3, 4], Ru/Cu/Ru [5], Ru [7], and RuCr [6] underlayers. Most of these films include Cu layers [1–5, 8, 9]. It is known that Cu atoms diffuse into Sm-Co film from underlayer and substitute the Co site in $SmCo_5$ structure forming an alloy compound of $Sm(Co,Cu)_5$. Cu dissolution is also known to stabilize 1:5 phase formation and to destabilize 2:17 phase formation [10–12].

The Co site in $SmCo_5$ structure can be replaced with other transition metal elements like Ni and CoNi [13]. $SmFe_5$ ordered phase, which is metastable and does not appear in the bulk phase diagram, has been prepared in the forms of film and powder samples [14–16]. The material showed a high magnetic anisotropy field of 40 kOe [16]. In order to investigate the film growth behavior during ordered phase formation, it is useful to prepare epitaxial films on single-crystal substrates by using a molecular beam epitaxy (MBE) system equipped with an *in-situ* reflection high-energy electron diffraction (RHEED) facility. However, there are very few reports on the formation of Sm-Fe epitaxial films. In our previous study [17], Sm-Fe films were MBE-grown on Cu(111) underlayers hetero-epitaxially grown on single-crystal substrates by varying the substrate temperature in a range between 300 and 500 °C. $SmFe_5$ ordered phase was formed above 350 °C. In the present study, Sm-Fe films were prepared on Cu(111) underlayers by varying the Sm/Fe composition from Fe-rich to Sm-rich region including $SmFe_5$ stoichiometry. The effects of film composition on the film growth and the film structure are investigated.

2 Experimental procedure

Thin films were prepared on MgO(111) single-crystal substrates at 500 °C by using an MBE system under base pressures lower than 7×10^{-9} Pa. Pure Cu (99.9999%), Sm (99.9%), and Fe (99.99%) were evaporated by using Knudsen cells. The film layer structure was Sm-Fe(20 nm)/Cu(20 nm)/MgO(111). 20-nm-thick Cu(111) underlayers were prepared through hetero-epitaxial growth on MgO(111) substrates. The epitaxial orientation relationship was determined by RHEED as Cu(111)[1$\bar{1}$0], (111)[$\bar{1}$ 10] || MgO(111)[1 $\bar{1}$ 0]. The Cu underlayers consisted of two fcc(111) variants whose atomic stacking sequences of close-packed plane along the perpendicular direction were ABCABC… and ACBACB… [18]. Sm and Fe were co-evaporated on the Cu underlayer and the thickness of Sm-Fe film was fixed at 20 nm. The composition of Sm-Fe film was varied from Fe-rich to Sm-rich region (10–30 at. % Sm) including almost $SmFe_5$ stoichiometry (17 at. % Sm).

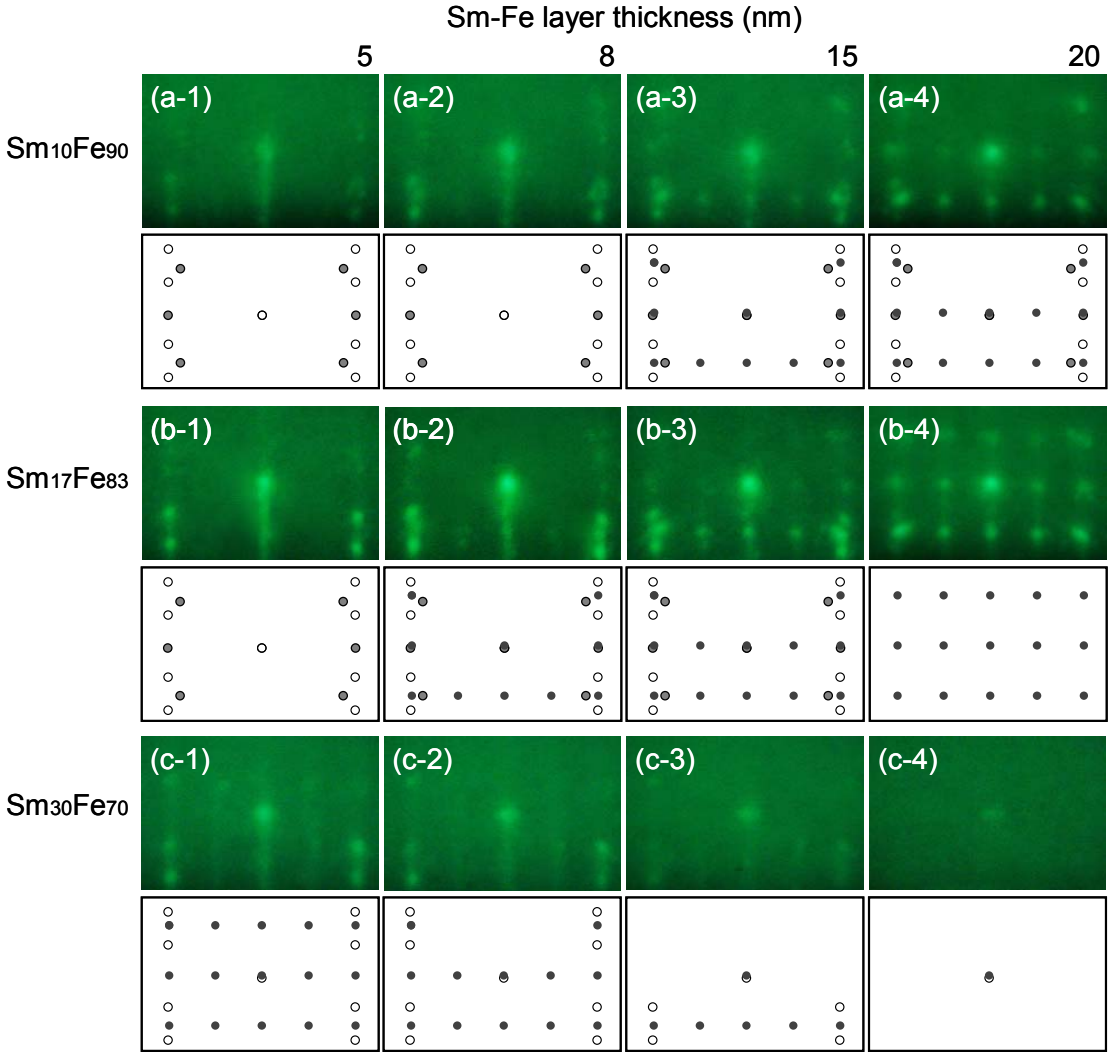

Fig. 1. RHEED patterns and the spot maps of (a) $Sm_{10}Fe_{90}$, (b) $Sm_{17}Fe_{83}$, and (c) $Sm_{30}Fe_{70}$ films deposited on Cu(111) underlayers. The film thicknesses are (a-1, b-1, c-1) 5, (a-2, b-2, c-2) 8, (a-3, b-3, c-3) 15, and (a-4, b-4, c-4) 20 nm. The incident electron beam is parallel to MgO[$1\bar{1}0$].

The surface structure during Sm-Fe deposition was studied by *in-situ* RHEED. The film structure was investigated by θ-2θ scan X-ray diffraction (XRD) with Cu-Kα radiation (λ = 0.15418 nm). The magnetization curves were measured by using a vibrating sample magnetometer.

3 Results and discussion

Figure 1(a) shows the RHEED patterns observed during formation of Sm-Fe film with the Sm composition of 10 at. %, which is an Fe-rich composition with respect to $SmFe_5$ stoichiometry. The RHEED patterns observed during the early stage of film formation [figures 1(a-1, a-2)] consist of spots corresponding to $Cu(111)_{fcc}$ and $Fe(110)_{bcc}$ reflections shown in the spot maps of figures 2(a) and (b). The RHEED pattern is also diffuse, which suggests that amorphous phase is involved in the film. This result indicates that Cu atoms diffuse from the underlayer into the Sm-Fe film and that amorphous-Sm and bcc-Fe phases are coexisting. This is possibly because the composition ratio of Sm to transition metals

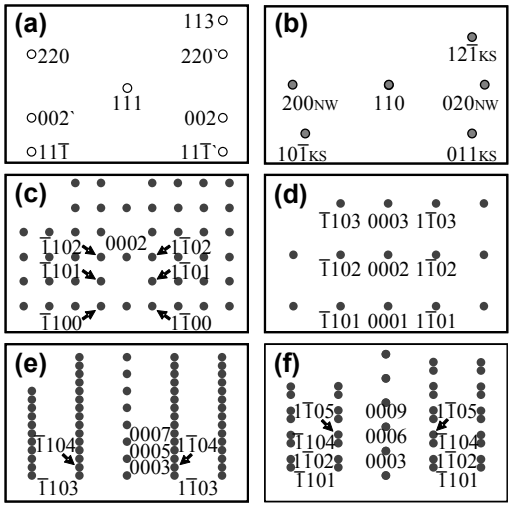

Fig. 2. RHEED spot maps simulated for (a) $Cu(111)_{fcc}$ and (b) $Fe(110)_{bcc}$ surfaces and (c)–(f) for Sm-Fe(0001) surfaces with (c) Th_2Ni_{17}-, (d) $CaCu_5$-, (e) Ce_2Ni_7-, and (f) $PuNi_3$-type structures. The incident electron beam is parallel to (a) Cu[$1\bar{1}0$]$_{fcc}$ and Cu[$\bar{1}10$]$_{fcc}$, (b) Fe[001]$_{NW}$ and Fe[$\bar{1}11$]$_{KS}$, or (f) Sm-Fe[$11\bar{2}0$].

(Fe and Cu) is much higher than 1:5 due to an influence of Cu atom diffusion from the underlayer. No Sm-Fe phases are formed at this growth stage. The epitaxial orientation relationships of Fe crystals with respect to Cu underlayer are determined by RHEED as follows,

$$\mathrm{Fe}(110)[001]_{\mathrm{bcc}} \parallel \mathrm{Cu}(111)[1\bar{1}0]_{\mathrm{fcc}} \quad \text{(type NW)},$$

$$\mathrm{Fe}(110)[\bar{1}11]_{\mathrm{bcc}} \parallel \mathrm{Cu}(111)[1\bar{1}0]_{\mathrm{fcc}} \quad \text{(type KS)}.$$

These orientation relationships are similar to the Nishiyama-Wassermann [19, 20] and the Kurdjumov-Sachs [21] relationships. With increasing the film thickness beyond 15 nm [figure 1(a-3)], a reflection corresponding to 1:5 ordered phase appears, as shown in the simulated RHEED spot maps of figures 2(c)–(f) and RHEED reflections from Cu and Fe crystals decreases. The reason is due to that the volume of Cu atoms diffused from the underlayer decreases with increasing the thickness and the ratio of Sm to transition metals (Fe and Cu) approaches to 1:5. By considering the Cu atom diffusion, an alloy compound of $Sm(Fe,Cu)_5$ is considered to be formed and the formation of metastable 1:5 phase is stabilized by partial replacements of Fe site with Cu atoms in the $SmFe_5$ structure. The crystallographic orientation relationship of

$$\mathrm{Sm(Fe,Cu)_5}(0001)[11\bar{2}0]_{\mathrm{CuCu5}} \parallel \mathrm{Cu}(111)[1\bar{1}0]_{\mathrm{fcc}}$$

is determined by RHEED. The $Sm(Fe,Cu)_5$ crystal is a single-crystal.

Figure 1(b) shows the RHEED patterns observed for an Sm-Fe film with the Sm composition of 17 at. %, which is almost $SmFe_5$ stoichiometry. In the early stage of film growth [figure 1(b-1)], the $Cu(111)_{fcc}$ and the $Fe(110)_{bcc}$ reflections are observed, similar to the case of $Sm_{10}Fe_{90}$ film. The reflection from 1:5 ordered phase appears with increasing the thickness beyond 8 nm [figure 1(b-2)], which is thinner than the thickness where the 1:5 ordered phase starts to be formed in the $Sm_{10}Fe_{90}$ film. This is due to that the ratio of Sm to transition metals (Fe and Cu) for $Sm_{17}Fe_{83}$ film is closer to 1:5 at this film growth stage than that for $Sm_{10}Fe_{90}$ film. As the thickness increases up to 20 nm [figure 1(b-4)], almost only the reflection from $Sm(Fe,Cu)_5$ ordered phase is recognized.

Figure 1(c) shows the RHEED patterns observed for an $Sm_{30}Fe_{70}$ film. The reflection from 1:5 ordered phase is observed from the early stage of film growth in addition to the $Cu(111)_{fcc}$ reflection. The reflection from bcc-Fe crystal is not observed, possibly due to that the $Fe_{30}Sm_{70}$ composition is an Sm-rich composition with respect to $SmFe_5$ stoichiometry. With increasing the film thickness, the clearness of RHEED pattern gradually decreases. The RHEED pattern variation suggests that an amorphous phase is appearing with increasing the film thickness. The reason is considered to be due to a lack of Cu atoms supplied from the underlayer which assist the formation of $Sm(Fe,Cu)_5$ ordered phase. From these experimental results, the compositional region where 1:5 ordered phase is formed is narrower in the $Sm(Fe,Cu)_5$ system, when compared with the cases of $Sm(Co,Cu)_5$ [8] and $Sm(Ni,Cu)_5$ [22] systems.

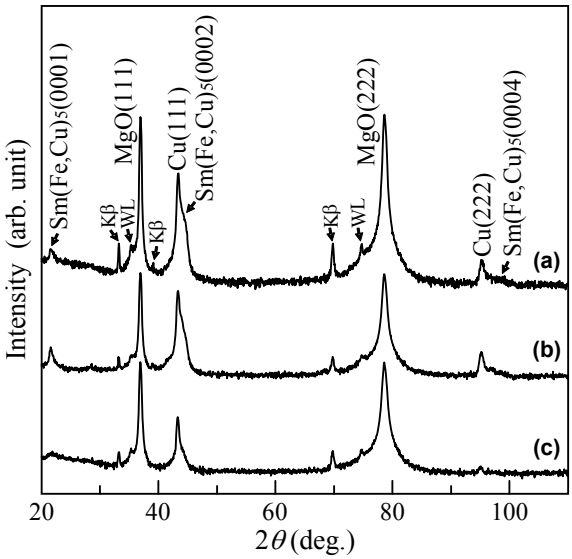

Fig. 3. XRD spectra of (a) $Sm_{10}Fe_{90}$, (b) $Sm_{17}Fe_{83}$, and (c) $Sm_{30}Fe_{70}$ films formed on Cu(111) underlayers. The intensity is shown in a logarithmic scale.

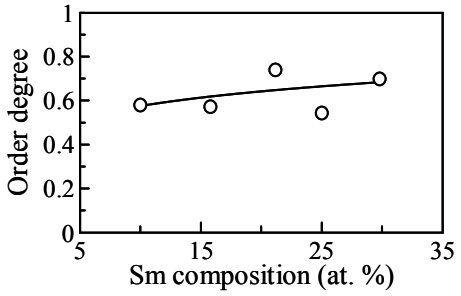

Fig. 4. Sm composition dependence on long-range order degree parameter.

Figure 3 shows the XRD of Sm-Fe films with different Sm/Fe compositions. (0001) superlattice reflections from $Sm(Fe,Cu)_5$ ordered phase are clearly observed around the diffraction angle, 2θ, of 22° in addition to (0002) and (0004) fundamental reflections for the investigated compositions. The intensity of Cu(111) reflection decreases with increasing the Sm composition, which suggests that the Cu atom diffusion is enhanced with increasing the Sm composition and a larger number of Cu atoms diffuse into the upper Sm-Fe film.

The long-range order degree (S) is calculated from the XRD data. The integrated intensity (I) is proportional to structure factor (F), Lorentz-polarization factor (L), absorption factor (A), and temperature factor (D) [23]. L and A are calculated by formulae,

$$L = (1 + \cos^2 2\theta)/(\sin^2\theta\cos\theta),$$

$$A = (1/2\mu) \times \{1 - \mathrm{e}^{-2\mu t/\sin\theta}\},$$

where μ and t are respectively the liner absorption coefficient and the film thickness. D is estimated from the date of $Sm(Fe,Cu)_5(0002)$ and $Sm(Fe,Cu)_5(0004)$ fundamental reflections. The intensity ratio of superlattice to fundamental reflection (I_s / I_f) is thus given by

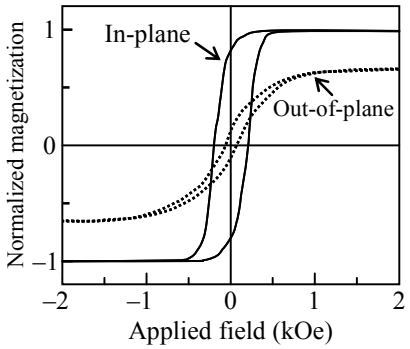

Fig. 5. Magnetization curves measured for an $Sm_{17}Fe_{83}$ film formed on Cu(111) underlayer.

$$(I_s/I_f) = (|F^2|LAD)_s/(|F^2|LAD)_f,$$

where the subscripts of s and f refer to the superlattice and the fundamental reflections, respectively. The $|F_s^2|$and the $|F_f^2|$ are respectively calculated to be

$$|F_s^2| = |F_{(0001)}{}^2| = |\{S(f_{Sm}-f_{Fe,Cu})\}^2|,$$

$$|F_f^2| = |F_{(0002)}{}^2| = |(f_{Sm}+5f_{Fe,Cu})^2|,$$

where f is atomic scattering factor. S is expressed by

$$S = [(I_s/I_f)\{(f_{Sm}+5f_{Fe,Cu})/(f_{Sm}-f_{Fe,Cu})\}^2\{(LAD)_f / (LAD)_s\}]^{1/2}.$$

Figure 4 shows the Sm composition dependence on S value. The S value is kept constant at around 0.55–0.75 regardless of Sm content.

Figure 5 shows the magnetization curves of $Sm_{17}Fe_{83}$ film formed on Cu(111) underlayer. The film shows an in-plane magnetic anisotropy. The magnetization property is apparently influenced by Cu atom diffusion from the underlayer. In the case of $Sm(Co,Cu)_5$ system, it is reported that the magnetic anisotropy decreases with increasing the Cu content. The $Sm_{17}Fe_{83}$ film prepared in the present study is composed of mixed phases consisting of $Sm(Fe,Cu)_5$ ordered phase with (0001) orientation and a small volume of bcc-Fe(110) phase.

4 Summary

Sm-Fe thin films are prepared on Cu(111) underlayers at 500 °C with varying the Sm composition from 10 to 30 at. %. The effect of Sm/Fe composition on the crystallographic properties is investigated. Formation of metastable $Sm(Fe,Cu)_5$ ordered phase is recognized in the investigated compositional range. Cu atoms diffuse from the underlayer into the Sm-Fe film and substitute the Fe site in $SmFe_5$ structure. The Sm-Fe films with Fe-rich compositions consist of $Sm(Fe,Cu)_5$ and bcc-Fe phases. On the other hand, the Sm-Fe films with Sm-rich compositions consist of $Sm(Fe,Cu)_5$ and amorphous phases. The Cu atom diffusion into Sm-Fe film plays an important role in assisting the formation of $Sm(Fe,Cu)_5$ ordered phase.

Acknowledgements

A part of this work was supported by MEXT-Japan and Hattori-Hokokai.

References

1. J. Sayama, T. Asahi, K. Mizutani, T. Osaka, J. Phys. D **37**, L1 (2004)
2. S. Takei, A. Morisako, M. Matsumoto, J. Magn. Magn. Mater. **272–276**, 1703 (2004)
3. J. Sayama, K. Mizutani, T. Asahi, J. Ariake, K. Ouchi, and T. Osaka, J. Magn. Magn. Mater. **301**, 271 (2006)
4. Y. K. Takahashi, T. Ohkubo, K. Hono, J. Appl. Phys. **100**, 053913 (2006)
5. I. Kato, S. Takei, X. Liu, A. Morisako, IEEE Trans. Magn. **42**, 2366 (2006)
6. X. Liu, H. Zhao, Y. Kubota, J. -P. Wang, J. Phys. D **41**, 232002 (2008)
7. M. Seifert, V. Neu, L. Schultz, Appl. Phys. Lett. **94**, 022501 (2009)
8. Y. Nukaga, M. Ohtake, F. Kirino, M. Futamoto, IEEE Trans. Magn. **44**, 2891 (2008)
9. M. Ohtake, Y. Nukaga, F. Kirino, M. Futamoto, J. Cryst. Growth **311**, 2251 (2009)
10. F. Hofer, IEEE Trans. Magn. **6**, 221 (1970)
11. K. Kamino, Y. Kimura, T. Suzuki, Y. Itayama, Trans. Jpn. Inst. Met. **14**, 135 (1973)
12. A. J. Perry, J. Less-Common Met. **51**, 153 (1977)
13. F. J. Cadieu, T. D. Cheung, S. H. Aly, L. Wickramasekara, R. G. Pirich, J. Appl. Phys. **53**, 8338 (1982)
14. F. J. Cadieu, T. D. Cheung, L. Wickramasekara, S. H. Aly, J. Appl. Phys. **55**, 2611 (1984)
15. T. S. Chin, C. H. Lin, H. J. Bai, Y. H. Huang, K. S. Cheng, S. H. Huang, IEEE Trans. Magn. **28**, 2587 (1992)
16. H. Oesterreicher, Appl. Phys. **15**, 341 (1978)
17. Y. Osamu, M. Ohtake, Y. Nukaga, F. Kirino, M. Futamoto, J. Phys.: Conf. Ser. **200**, 082026 (2010)
18. M. Ohtake, K. Kobayashi, M. Futamoto, IEEE Trans. Magn. (2012)
19. G. Wassermann, Arch. Eisenhuettenwes **16**, 647 (1933)
20. Z. Nishiyama, Sci. Rep. Tohoku Univ. **23**, 638 (1934)
21. G. Kurdjumov, G. Sachs, Z. Phys. **64**, 325 (1930)
22. T. Yanagawa, M. Ohtake, D. Suzuki, F. Kirino, M. Futamoto, Proc. REPM 2012.
23. B. D. Cullity, in *Elements of X-Ray Diffraction* (Addsion-Wesley, Massachusetts, 1956) pp. 104–137